

Achievable capacity improvement by using multi-level modulation format in trench-assisted multi-core fiber system

J. H. Chang, H. G. Choi, and Y. C. Chung*

Department of Electrical Engineering, Korea Advanced Institute of Science and Technology 335 Gwahangno, Yuseong-gu, Daejeon 305-701, South Korea
ychung@ee.kaist.ac.kr

Abstract: We evaluate the impacts of using multi-level modulation formats on the transmission capacity of the multi-core fiber (MCF) having trench-assisted index profile and hexagonal layout. For this evaluation, we utilize the spectral efficiency per unit area, defined as the spatial spectral efficiency (SSE). The results show that the SSE improvement achievable by using the higher-level modulation format can be reduced due to its lower tolerance to the inter-core crosstalk. We also evaluate the effects of using large effective area on the transmission capacity of the trench-assisted MCF. The results show that the use of large effective area can decrease this capacity due to the increased inter-core crosstalk and lengthened cable cutoff wavelength, although it can help increase the transmission distance. Thus, it is necessary to optimize the effective area of MCF by considering both the SSE and transmission distance. However, the results indicate that the effect of using different effective areas on the SSE-distance product is not significant, and it is not useful to increase the effective area of the trench-assisted MCF to be larger than $\sim 110 \mu\text{m}^2$.

©2013 Optical Society of America

OCIS codes: (060.2330) Fiber optics communications; (060.4080) Modulation.

References and links

1. S. Randel, R. Ryf, A. Sierra, P. J. Winzer, A. H. Gnauck, C. A. Bolle, R.-J. Essiambre, D. W. Peckham, A. McCurdy, and R. Lingle, Jr., "6×56-Gb/s mode-division multiplexed transmission over 33-km few-mode fiber enabled by 6×6 MIMO equalization," *Opt. Express* **19**(17), 16697–16707 (2011).
2. T. Morioka, "New generation optical infrastructure technologies: "EXAT initiative" towards 2020 and beyond," in *Proc. OptoElectron. Commun. Conf. (OECC)* (2009), paper FT4.
3. T. Morioka, Y. Awaji, R. Ryf, P. Winzer, D. Richardson, and F. Poletti, "Enhancing optical communications with brand new fibers," *IEEE Commun. Mag.* **50**(2), S31–S42 (2012).
4. J. Sakaguchi, B. J. Puttnam, W. Klaus, Y. Awaji, N. Wada, A. Kanno, T. Kawanishi, K. Imamura, H. Inaba, K. Mukasa, R. Sugizaki, T. Kobayashi, and M. Watanabe, "19-core fiber transmission of 19×100×172-Gb/s SDM-WDM-PDM-QPSK signals at 305Tb/s," in *Proc. Optical Fiber Commun. Conf. (OFC)* (2011), paper PDP5C.1.
5. R. Ryf, R.-J. Essiambre, S. Randel, A. H. Gnauck, P. J. Winzer, T. Hayashi, T. Taru, and T. Sasaki, "MIMO-based crosstalk suppression in spatially multiplexed 3×56-Gb/s PDM-QPSK signals for strongly coupled three-core fiber," *IEEE Photon. Technol. Lett.* **23**(20), 1469–1471 (2011).
6. T. Hayashi, T. Sasaki, and E. Sasaoka, "Multi-core fibers for high capacity transmission," in *Proc. Optical Fiber Commun. Conf. (OFC)* (2012), paper OTu1D4.
7. K. Takenaga, T. Arakawa, S. Tanigawa, N. Guan, S. Matsuo, K. Saitoh, and M. Koshihara, "Reduction of crosstalk by trench-assisted multi-core fiber," in *Proc. Optical Fiber Commun. Conf. (OFC)* (2011), paper OWJ4.
8. K. Takenaga, Y. Arakawa, Y. Sasaki, S. Tanigawa, S. Matsuo, K. Saitoh, and M. Koshihara, "A large effective area multi-core fiber with an optimized cladding thickness," *Opt. Express* **19**(26), B543–B550 (2011).
9. T. Hayashi, T. Taru, O. Shimakawa, T. Sasaki, and E. Sasaoka, "Design and fabrication of ultra-low crosstalk and low-loss multi-core fiber," *Opt. Express* **19**(17), 16576–16592 (2011).
10. T. Hayashi, T. Taru, O. Shimakawa, T. Sasaki, and E. Sasaoka, "Low-loss and large- A_{eff} multi-core fiber for SNR enhancement," in *Proc. European Conf. on Opt. Commun. (ECOC)* (2012), paper Mo.1.F.3.

11. M. Koshiba, K. Saitoh, K. Takenaga, and S. Matsuo, "Analytical expression of average power-coupling coefficients for estimating intercore crosstalk in multicore fibers," *IEEE Photon. J.* **4**(5), 1987–1995 (2012).
12. T. Hayashi, T. Sasaki, E. Sasaoka, K. Saitoh, and M. Koshiba, "Physical interpretation of intercore crosstalk in multicore fiber: effects of macrobend, structure fluctuation, and microbend," *Opt. Express* **21**(5), 5401–5412 (2013).
13. P. J. Winzer, A. H. Gnauck, A. Konczykowska, F. Jorge, and J.-Y. Dupuy, "Penalties from in-band crosstalk for advanced optical modulation formats," in *Proc. European Conf. on Opt. Commun. (ECOC)* (2011), paper Tu.5.B.7.
14. K.-P. Ho, "Effects of homodyne crosstalk on dual-polarization QPSK signals," *IEEE J. Lightw. Technol.* **29**(1), 124–131 (2011).
15. S. Mumtaz, R.-J. Essiambre, and G. P. Agrawal, "Reduction of nonlinear penalties due to linear coupling in multicore optical fibers," *IEEE Photon. Technol. Lett.* **24**(18), 1574–1576 (2012).
16. P. J. Winzer, A. H. Gnauck, C. R. Doerr, M. Magarini, and L. L. Buhl, "Spectrally efficient long-haul optical networking using 112-Gb/s polarization-multiplexed 16-QAM," *IEEE J. Lightw. Technol.* **28**(4), 547–556 (2010).
17. B. Zhu, J. M. Fini, M. F. Yan, X. Liu, S. Chandrasekhar, T. F. Taunay, M. Fishteyn, E. M. Monberg, and F. V. Dimarcello, "High-capacity space-division-multiplexed DWDM transmissions using multicore fiber," *J. Lightwave Technol.* **30**(4), 486–492 (2012).
18. S. Chandrasekhar, A. H. Gnauck, X. Liu, P. J. Winzer, Y. Pan, E. C. Burrows, T. F. Taunay, B. Zhu, M. Fishteyn, M. F. Yan, J. M. Fini, E. M. Monberg, and F. V. Dimarcello, "WDM/SDM transmission of 10 x 128-Gb/s PDM-QPSK over 2688-km 7-core fiber with a per-fiber net aggregate spectral-efficiency distance product of 40,320 km·b/s/Hz," *Opt. Express* **20**(2), 706–711 (2012).

1. Introduction

To overcome the imminent capacity limit of the conventional single-mode fiber (SMF), there have recently been many efforts to realize the space-division-multiplexing (SDM) technology [1–4]. In particular, there have been many attempts to develop the multi-core fiber (MCF) in the hope of increasing the capacity of a single strand of fiber in proportion to the number of cores used in it [2–4]. In order to maximize the capacity of MCF, it is necessary to increase the core density per unit area. However, as we reduce the inter-core distance, the inter-core crosstalk is increased. This increased crosstalk can hinder the use of the spectrally efficient high-level modulation format, which is also critical to maximize the capacity of MCF, since the higher-level modulation format is more sensitive to the crosstalk. Thus, the capacity of MCF may not be maximized simply by reducing the inter-core distance to increase the core density. In principle, this problem can be solved by using the multiple-input multiple-output (MIMO) signal processing technique [5]. However, this technique requires the use of heavy computational resources. In addition, in the all-optical networks implemented with a large number of optical add/drop multiplexers, it may be difficult to solve this inter-core crosstalk problem by using MIMO technique. This is because, in such a network, the received signals can be contaminated with different inter-core crosstalk components originating from different sections of the MCF link.

The performances of the high-speed optical signals in the MCF transmission system can also be affected by the fiber nonlinearities, as in the conventional SMF system. It is well known that the higher-level modulation format is more vulnerable to these nonlinearities. Thus, to facilitate the use of the high-level format in the MCF system, one may think that it is desirable to increase the effective area of each core. However, as we increase the effective area, the inter-core crosstalk can also be increased due to the increased mode-field diameter (MFD) [6]. As a result, the capacity of MCF may not be increased as expected by increasing the effective area of each core.

In this paper, we evaluate the impacts of using the high-level modulation formats on the capacity of MCF. In this evaluation, we assume that a weakly coupled MCF fabricated with a trench-assisted index profile is used as a transmission fiber. We then evaluate the effects of the inter-core crosstalk on the performances of the SDM signals modulated in various types of multi-level formats such as the quadrature phase-shift keying (QPSK), 16 quadrature amplitude modulation (16QAM), and 64QAM. As expected, it is necessary to increase the inter-core distance (and sacrifice the spatial efficiency) for the utilization of the higher-level

format due to its lower tolerance to the inter-core crosstalk. Thus, we evaluate the spectral efficiency (SE) per unit area, defined as the spatial spectral efficiency (SSE), achievable by using each modulation format. The results show that the SSE of the 100-km long MCF transmission system can be increased by a factor of only ~ 2.3 by using the 64QAM format instead of the QPSK format, while it is 3 in the conventional SMF system. This improvement is further reduced as the transmission distance is increased. We also estimate the impacts of increasing the effective area of each core on the SSE of MCF. For this purpose, we assume the use of MCFs having various effective areas in the range of $75 \sim 130 \mu\text{m}^2$, and estimate the SSE improvement achievable by using the high-level formats. The results show that the use of the large effective area in the MCF is not as efficacious as in the conventional SMF for increasing the fiber capacity, since it increases the cable cutoff wavelength as well as the inter-core crosstalk.

2. Minimum core pitch of MCF required for the transmission of multi-level signals

The most important sources of the performance degradation in the MCF transmission system are the inter-core crosstalk and fiber nonlinearities. Thus, the MCF should be designed to avoid these problems. Recently, it has been reported that the MCF with trench-assisted index profile is quite effective in satisfying these requirements compared to the one with step-index profile [4], [6–10]. Thus, we first focused our evaluation on such a MCF described in [7]. Figure 1 shows the index profile of the trench-assisted MCF. The geometrical parameters of this MCF, d_1 , d_2 , d_3 , Δ_1 , and Δ_2 were $8.2 \mu\text{m}$, $18.3 \mu\text{m}$, $26.5 \mu\text{m}$, 0.38% , and -0.65% , respectively. Accordingly, we assumed that the effective area, chromatic dispersion, and dispersion slope of each core in the MCF were $75 \mu\text{m}^2$, 18 ps/nm/km , and $0.09 \text{ ps/nm}^2/\text{km}$, respectively, at the wavelength of 1550 nm .

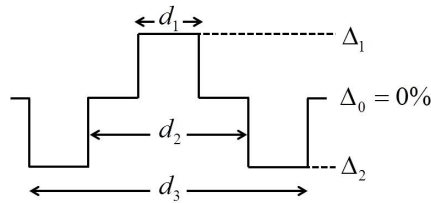


Fig. 1. Refractive-index profile of the trench-assisted MCF.

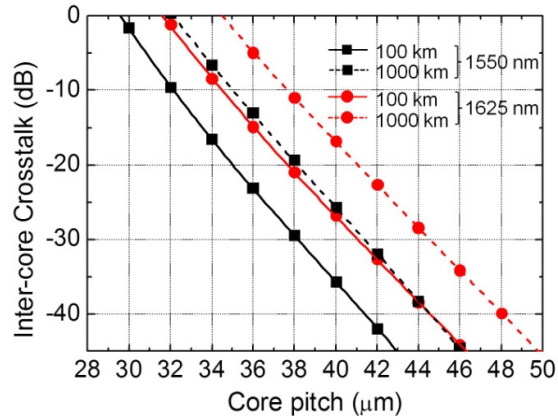


Fig. 2. Inter-core crosstalk level estimated as a function of the core pitch in the MCF with trench-assisted index profile [7]. The operating wavelength was assumed to be either 1550 nm or 1625 nm .

To estimate the inter-core crosstalk level, we initially evaluated the coupling coefficient between two cores in the MCF as a function of the core pitch by using the full-vector beam

propagation method (BPM). We then calculated the crosstalk level under the bending condition [9], [11,12]. In this calculation, we assumed that the bending radius was 100 mm and the signal's wavelength was either 1550 nm or 1625 nm. Figure 2 shows the crosstalk level at the core surrounded by six other cores (i.e., the worst case) calculated as a function of the core pitch for a homogeneous MCF with hexagonal layout. In this figure, the inter-core crosstalk in the y-axis represents the sum of the mean crosstalk from six neighboring cores. It should be noted that, when the MCF was designed to have multiple cores in the hexagonal layout, the crosstalk from other than these six cores in the most proximate layer could be neglected. The results also show that the inter-core crosstalk becomes larger by ~ 10 dB at 1625 nm than the value at 1550 nm due to the larger MFD at the longer wavelength. We confirmed that these values were similar to those reported in [7].

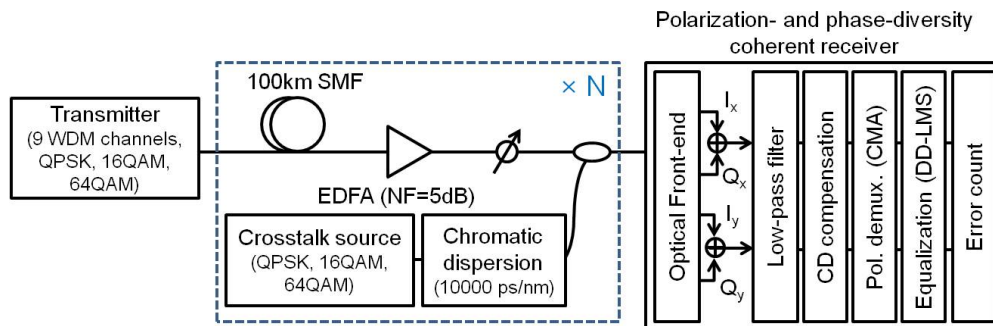


Fig. 3. Simulation model used to evaluate the performance degradation in the MCF link. The WDM signals were modulated in the PDM-QPSK, PDM-16QAM, or PDM-64QAM format.

Figure 3 shows the simulation model used to evaluate the effect of the inter-core crosstalk and fiber nonlinearities on the performances of the MCF transmission system. This model is based on the experimental setup used to evaluate the impacts of the in-band crosstalk in [13]. We considered 9 wavelength-division-multiplexed (WDM) signals modulated either in the polarization-division-multiplexed (PDM)-QPSK, PDM-16QAM, or PDM-64QAM format at 112 Gb/s. For the generation of these signals, we assumed that the dual-nested Mach-Zehnder modulators driven by non-return-to-zero (NRZ) signals were used. These modulated signals were first filtered by using the 4th-order super-Gaussian filter (3-dB bandwidth: 90% of the channel spacing) to minimize the effects of the inter-channel crosstalk and inter-symbol interference (ISI). We then multiplexed these signals by using an optical coupler. The channel spacings of these WDM signals modulated in PDM-QPSK, PDM-16QAM, and PDM-64QAM formats were assumed to be 50.0 GHz, 25.0 GHz, and 16.7 GHz, respectively. Thus, the SEs of these signals were 2 b/s/Hz, 4 b/s/Hz, and 6 b/s/Hz, respectively. We also assumed that these 9 WDM signals were coupled into the center core of the MCF. However, for the simplicity of the numerical simulations, we used an SMF link in this model and emulated the effects of the inter-core crosstalk occurred in the MCF by using an additional crosstalk source. Thus, the crosstalk level could be adjusted simply by changing the power ratio between the WDM signals and crosstalk source. However, it has been reported that the amplitude of the combined crosstalk from multiple sources (i.e., six neighboring cores in our case) has Gaussian distribution [14]. Thus, to evaluate the effect of the inter-core crosstalk occurred in each MCF span by using single crosstalk source, we placed a dispersive element (dispersion: 10,000 ps/nm) at the output of the crosstalk source (so that its amplitude could also have Gaussian distribution). We also assumed that the effect of fiber nonlinearities in the MCF was identical to that in the SMF (since the intermodal nonlinear coupling between the spatial modes in different cores is much smaller than the intramodal nonlinear coupling as long as the core pitch of MCF is sufficiently large ($>30 \mu\text{m}$) [15]). The transmission link was assumed to be consisted of 100-km long spans. The span loss of 20 dB was fully compensated

by an Erbium-doped fiber amplifier (EDFA), which had a noise figure of 5 dB. Thus, the amplified spontaneous emission (ASE) noise was added at each span. No dispersion compensating module was used in this transmission link. We estimated the performance of the center channel among 9 WDM channels by using a digital coherent receiver. At the receiver, we first demultiplexed the WDM channel by using an optical filter (which was identical to the one used at the transmitter's site). The demultiplexed channel was then detected by using a polarization- and phase-diversity homodyne coherent receiver. We resampled the detected electrical signals at 2 samples per symbol and applied a low-pass filter (4th-order Bessel filter, 3-dB bandwidth: 70% of the symbol rate). The dispersion compensation was achieved by using a finite impulse response (FIR) filter. For the polarization demultiplexing, we processed the sampled signals by using a MIMO equalizer [16]. The pre-convergence was achieved by using 15-tap, T/2-spaced adaptive FIR filter based on the constant modulus algorithm (CMA). We then used the decision-directed least-mean-square (DD-LMS) method for the equalization and calculated the bit-error-rate (BER).

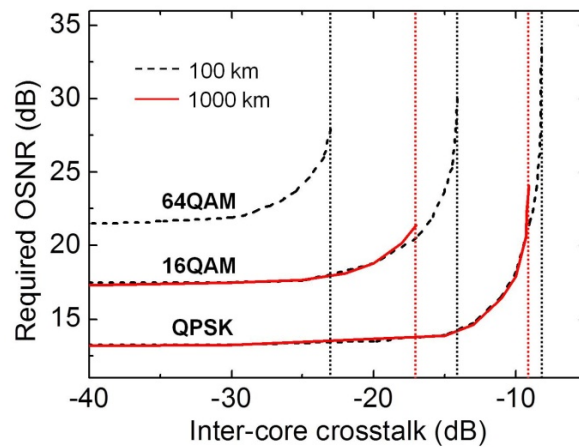


Fig. 4. Required OSNRs to achieve the BER better than the FEC limit (i.e., $\text{BER} = 3.8 \times 10^{-3}$) as a function of the inter-core crosstalk for various modulation formats such as PDM-QPSK, PDM-16QAM and PDM-64QAM. The transmission distance was either 100 km or 1000 km.

Using this model, we estimated the required OSNR to achieve the BER better than the forward-error correction (FEC) limit (i.e., $\text{BER} = 3.8 \times 10^{-3}$) as a function of the inter-core crosstalk level in the 100-km and 1000-km long MCF links. Figure 4 shows the results. As we increased the crosstalk level, the required OSNR was also increased regardless of the modulation format. However, after the inter-core crosstalk reached a certain level, it was no longer possible to achieve the BER below the FEC limit even if we further increased the signal's power (i.e., OSNR) due to the effects of fiber nonlinearities. From this result, we obtained the maximum allowable crosstalk level for each modulation format (shown by the vertical dotted lines in Fig. 4). This crosstalk level was used to compare the effects of using various multi-level formats on the achievable capacity of MCF. As expected, the higher-level modulation format had worse tolerance to the crosstalk. Using the results in Figs. 2 and 4, we estimated the minimum core pitches required to achieve the BER better than the FEC limit using various modulation formats. However, it should be noted that the larger core pitch is required to accommodate the signals operating at the longer wavelengths. Thus, it is necessary to design the core pitch to be large enough to support the longest wavelength used in the MCF. In this estimation, we assumed that the longest wavelength was 1625 nm (i.e., the upper limit of the L-band). The results showed that, when the transmission distance was 100 km, the required core pitches were 34.0, 35.8, and 38.7 μm for the QPSK, 16QAM and 64QAM signals, respectively. However, when we extended the transmission distance to 1000

km, these values were increased to 37.3 and 40.2 μm for the QPSK and 16QAM signals, respectively. It was not possible to transmit the 64QAM signal over 1000 km even in the absence of the inter-core crosstalk due to its high OSNR requirement.

3. Achievable spatial spectral efficiency of MCF transmission system

Although we can achieve the higher SE by using the higher-level modulation format, its use requires a larger core pitch of MCF, which, in turn, leads to the lower spatial efficiency. Thus, in case of using MCF, it may not be possible to maximize the total fiber capacity per unit area by using the higher-level format. Thus, to evaluate the actual fiber capacity achievable by using the high-level format in the MCF transmission system, both the spectral and spatial efficiencies should be considered. For this purpose, we defined the SSE as $(SE/core) \times (N/A)$, where N is the number of cores in the MCF and A is the transverse area of MCF. We assumed that the cores were arranged in hexagonal layout and the thickness of the outermost cladding was identical to the core pitch. Thus, A could be approximated by $C \times N \times (\pi\Lambda^2)$, where Λ is the core pitch of the MCF and the constant C is equal to $(4/3)^2/3$, $(6/5)^2/3$, and $(8/7)^2/3$ for the 7-, 19-, and 37-core MCFs, respectively. Using these parameters, we evaluated the improvement of SSE (i.e., the fiber capacity per unit area) achievable by using the high-level format in the MCF transmission system. For example, we first evaluated this SSE improvement achievable in the 100-km and 1000-km long MCF links by using the minimum core pitches estimated in the previous section. Figure 5(a) shows the results for 7-core MCF. In the case of the conventional SMF link, the SSE increases linearly with the number of bits used in a symbol. However, in the case of the MCF link, the SSE improvement obtained by using the higher-level format was significantly smaller than that in the SMF link due to the inter-core crosstalk. For example, even when the transmission distance was only 100 km, the SSE improvement obtained by using the 16QAM format instead of the QPSK format in the MCF link was reduced by $\sim 20\%$ compared to the achievable value in the SMF link. This effect was worse for the 64QAM format since the SSE was improved by only $\sim 130\%$ (instead of 200% achievable in the SMF link).

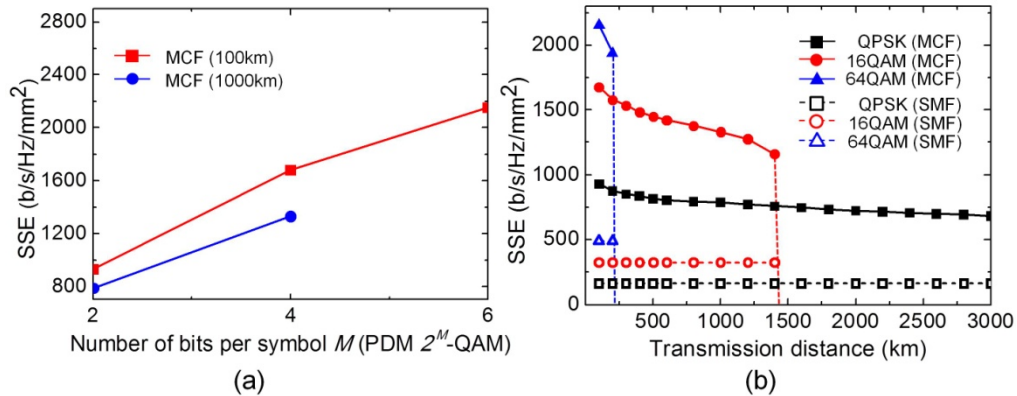


Fig. 5. (a) Spatial spectral efficiency (SSE) of 7-core MCF achievable by using various formats such as PDM-QPSK, PDM-16QAM, and PDM-64QAM. (b) Spatial spectral efficiencies (SSEs) of 7-core MCF as a function of the transmission distance for 112-Gbps PDM-QPSK, PDM-16QAM, and PDM-64QAM signals. The SSEs of the conventional SMF are also shown as references.

We also investigated the dependency of the achievable SSE on the transmission distance in the MCF link. For this purpose, we evaluated the SSE as a function of the number of spans. In this evaluation, every data was calculated by using its optimum launch power. For example, when the transmission distance was 1000 km, the optimum launch powers for the QPSK and 16QAM signals were 0 dBm and -2 dBm, respectively. Figure 5(b) shows the

results. In this figure, we included the SSEs of the conventional SMF (i.e., cladding diameter: 125 μm) as references. As we increased the transmission distance of the MCF link, the inter-core crosstalk was accumulated as well as the amplified spontaneous emission (ASE) noises. Thus, to achieve the BER better than the FEC limit even after the long-distance transmission, it was necessary to utilize a large core pitch (which would inevitably reduce the spatial efficiency). As a result, the SSE was gradually deteriorated with the transmission distance. However, we noted that the SSE of the higher-level signal was deteriorated more rapidly than that of the lower-level signal. For example, in the case of using the QPSK signals, the core pitch should be increased from 34.0 μm to 37.3 μm to achieve the BER performance better than the FEC limit even after increasing the transmission distance from 100 km to 1000 km. However, in the case of using the 16QAM signals, the core pitch should be increased from 35.8 μm to 40.2 μm for the same purpose. These results indicated that the SSE improvement achievable by using the higher-level format deteriorated more rapidly with the increased transmission distance. For example, in the case of the 100-km long MCF link, the SSE could be improved by $\sim 80\%$ by using the 16QAM signals instead of the QPSK signals, regardless of the number of cores. However, this SSE improvement was reduced to $\sim 53\%$ when the transmission distance was increased to 1400 km.

To check the validity of our SSE estimation, we compared our results with the previously reported experimental values. For example, in [17], the PDM-QPSK signals were transmitted over 76.8-km long MCF link having a core pitch of 46.8 μm and step-index profile. We estimated the maximum SSE achievable in this system by using the same parameters reported in this paper. The results showed that our estimated value (~ 664 b/s/Hz/mm²) was somewhat larger than the SSE extracted from their experimental results (~ 490 b/s/Hz/mm²). However, they could extend their transmission distance to 2688 km by using the same MCF [18]. In this case, their experimental result (~ 490 b/s/Hz/mm²) became comparable to our estimated value (~ 512 b/s/Hz/mm²).

4. Impact of increased effective area on the SSE of trench-assisted MCF

In the conventional SMF transmission system, the limitations imposed by fiber nonlinearities can be mitigated by increasing the fiber's effective area. However, when the MCF is used, the inter-core crosstalk can also be increased as we increase the effective area of each core. Thus, the capacity of MCF may not be increased as expected by increasing its effective area. To resolve this problem and evaluate the effects of the increased effective area on the SSE of the MCF, we considered three types of MCFs having the trench-assisted index profile. Table 1 shows the parameters of these MCFs as well as their resulting effective areas. We designated the MCFs having the effective areas of 75 μm^2 , 110 μm^2 , and 130 μm^2 as MCF A, MCF B, and MCF C, respectively. MCF A and MCF B were identical to the MCFs reported in [7,8], and MCF C was similar to the MCF reported in [10]. Figure 6(a) shows the inter-core crosstalk levels calculated as a function of the core pitch for these MCFs. In this calculation, the signal's wavelength was assumed to be 1625 nm. The results showed that, if we utilized MCF B and MCF C instead of MCF A, the core pitch should be increased by ~ 1 μm and ~ 7 μm , respectively, to maintain the crosstalk to be < -20 dB.

Table 1. Parameters of various trench-assisted MCFs

Parameter	MCF A	MCF B	MCF C
d_1 (μm)	8.2	10.3	12.8
d_2 (μm)	18.3	22.2	21.2
d_3 (μm)	26.5	32.0	26.0
Δ_1 (%)	0.38	0.26	0.26
Δ_2 (%)	-0.65	-0.70	-0.56
A_{eff} (μm^2)	75	110	130

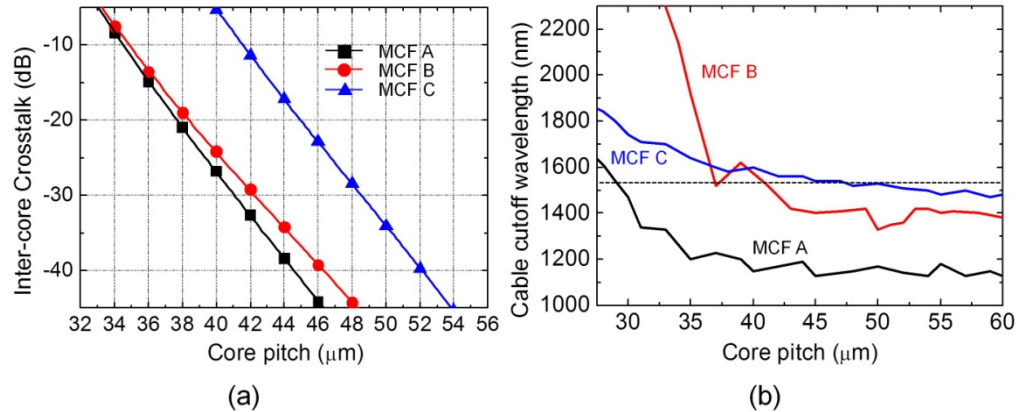


Fig. 6. (a) Inter-core crosstalk level estimated as a function of the core pitch for three types of 7-core MCFs. The operating wavelength and transmission distance were assumed to be 1625 nm and 100 km, respectively. (b) Cable cutoff wavelength as a function of the core pitch for three types of 7-core MCFs.

On the other hand, it is well known that the cable cutoff wavelength of the optical fiber tends to be increased as we increase its effective area. In addition, in the case of the trench-assisted MCF with hexagonal layout, the cable cutoff wavelength of the center core (or the core surrounded by six neighboring cores) can also be shifted to the longer wavelength due to the additional confinement of the higher-order modes by the trench layers of the neighboring cores (especially when the core pitch is small) [8]. As a result, the single-mode operation of the core surrounded by six neighboring cores in the MCF cannot be guaranteed at the short wavelength as we increase the effective area. For example, Fig. 6(b) shows the relationship between the cable cutoff wavelengths of the center cores and the core pitches of the MCFs described in Table 1. In general, the cable cutoff wavelength was increased as we increased the effective area of the MCF. However, when the core pitch was smaller than 40 μm , MCF C had shorter cutoff wavelength than MCF B despite its larger effective area. This was because MCF C was designed to have a relatively narrow trench (i.e., its width was only 4.8 μm). As a result, when the core pitch was small, the effect of the additional confinement on the cable cutoff wavelength became less significant in MCF C than in MCF B (which had a trench width of 9.8 μm). However, it would be impractical to reduce the core pitch of MCF C to be less than 40 μm due to the unacceptably large inter-core crosstalk generated at such a short core pitch. Thus, in order to ensure the single-mode operation at 1530 nm (i.e., the shortest wavelength in the C-band), the core pitch should be larger than 29 μm , 41 μm , and 50 μm for MCF A, MCF B, and MCF C, respectively, as shown in Fig. 6(b). These results indicated that this minimum core pitch requirement (to ensure the single-mode operation even at the short wavelength) could also drastically reduce the spatial efficiency of MCF C (i.e., the MCF with large effective area), while it had little impact on the MCF A. Thus, we inferred that the use of the large effective area could hinder the realization of the densely spaced cores in the MCF, although it might help extending the transmission distance to some extent. To illustrate this point, we estimated the SSEs of three MCFs in Table 1 as a function of the transmission distance and modulation format. For this estimation, we optimized the SSE for each transmission distance with respect to the inter-core crosstalk, ASE, and nonlinear impairments. Figure 7 shows the results. As we increased the effective area of each core in the MCF, the SSE was deteriorated for every modulation format due to the increased inter-core crosstalk and cable cutoff wavelength. However, by increasing the effective area (thus, mitigating the effects of fiber nonlinearities), we could somewhat extend the transmission distance at the cost of the sacrificed SSE. For example, the maximum transmission distance of the 16QAM signal could be increased from 1400 km to 2000 km by utilizing MCF C instead

of MCF A. However, in the 2000-km long transmission system, the SSE achievable by using the 16QAM signals and MCF C was similar to the value achievable by using the QPSK signals and MCF A. Thus, it would be necessary to optimize the effective area of each core in the MCF by considering both the SSE and required transmission distance. For this purpose, we evaluated the SSE-distance products achievable by using various types of the modulation formats in the fiber links implemented by using MCF A, MCF B, and MCF C. The results in Fig. 8 showed that the improvement of the SSE-distance product achieved by increasing the effective area of each core in the MCF was not significant regardless of the modulation formats. For example, when we utilized the QPSK signals, the SSE-distance product could be improved by only ~11% by using MCF B instead of MCF A. However, when we further increased the effective area (by utilizing MCF C), the SSE-distance product became reduced compared to the case of using MCF A due to the drastically increased inter-core crosstalk and cable cutoff wavelength.

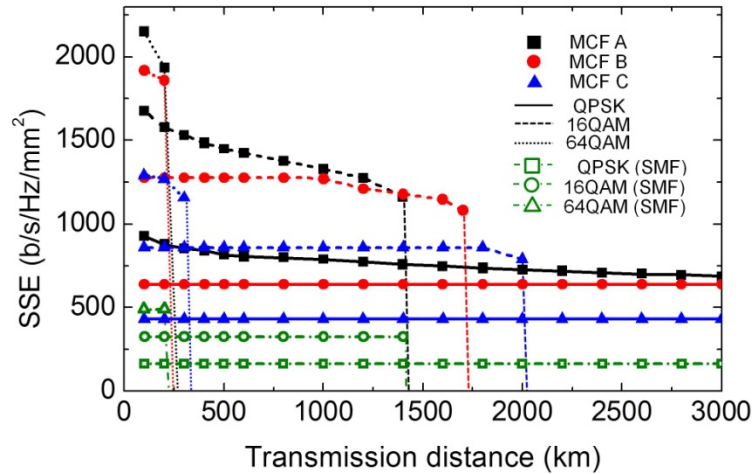


Fig. 7. Spatial spectral efficiencies (SSEs) of three types of 7-core MCFs (having different effective areas) achievable by using PDM-QPSK, PDM-16QAM, and PDM-64QAM formats. The SSEs of the conventional SMF are also shown as references.

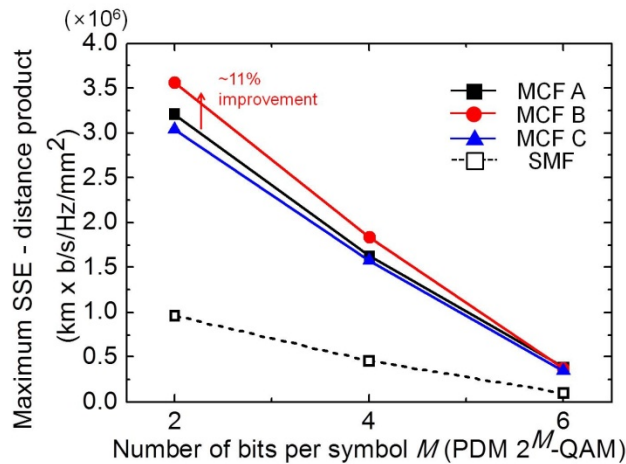


Fig. 8. Maximum SSE-distance products of 7-core MCFs achievable by using various formats such as PDM-QPSK, PDM-16QAM, and PDM-64QAM. The values for the conventional SMF (dashed line) are also shown as references.

It would be highly desirable if we could optimize the design of the trench-assisted MCF to have the large effective area, low inter-core crosstalk, and acceptable cable cutoff wavelength simultaneously. However, it appears to be a difficult task. In order to suppress the inter-core crosstalk in the trench-assisted MCF, it was necessary to increase the index difference of the trench. However, this increased index difference of the trench could also increase the effective index difference between the core and cladding and, as a result, reduce the effective area. We could of course suppress the inter-core crosstalk without this problem by increasing the width of the trench or the spacing between the core and trench layer. However, in this case, the cable cutoff wavelengths of the neighboring cores could be increased. Thus, there was a trade-off between the inter-core crosstalk and the cable cutoff wavelength for the design of the MCF having large effective area. In other words, the spatial efficiency improvement achievable by designing the MCF to have low inter-core crosstalk (i.e., by increasing the width of the trench) could be negated by the increased core pitch required to support the shortest wavelength used in the system. Thus, we concluded that the optimum effective area for maximizing the SSE-distance product was $\sim 110 \mu\text{m}^2$ for the trench-assisted MCF.

5. Summary

We evaluated the effects of using multi-level modulation formats on the transmission capacity of the MCF having trench-assisted index profile and hexagonal layout. To maximize this capacity, it would be vital to utilize the multi-level modulation formats. However, since the higher-level format was more sensitive to the inter-core crosstalk, it was indispensable to utilize the larger core pitch in the MCF for the transmission of the signals modulated in such a format. This would inevitably deteriorate the spatial efficiency. As a result, the ultimate fiber capacity per unit area achievable by using the high-level format in the MCF transmission system was smaller than expected. For example, in the 500-km long MCF link, the SSE improvement by using 16QAM signals instead of QPSK signals was estimated to be only $\sim 75\%$ (instead of 100% achievable in the conventional SMF link). This tendency became more serious as the transmission distance was increased. For example, this SSE improvement was reduced to $\sim 53\%$ when the distance was increased to 1400 km. We also evaluated the effects of increasing the effective area on the transmission capacity of the trench-assisted MCF. When we increased the effective area of each core in such an MCF, not only the inter-core crosstalk was increased but also the cable cutoff wavelength was shifted to the longer wavelength. To overcome these problems, it was necessary to increase the core pitch of MCF, which, in turn, deteriorated the spatial efficiency. As a result, the use of large effective area in the MCF was detrimental for maximizing its capacity, although it could help increasing the transmission distance. Thus, it would be necessary to optimize the effective area of each core in the MCF by considering both the SSE and transmission distance. For this purpose, we evaluated the SSE-distance products achievable by using various types of the modulation formats in the transmission links implemented by using MCFs with various effective areas. The results showed that we could achieve the largest SSE-distance product by using MCF B, indicating that there might be no need to increase the effective area of the trench-assisted MCF to be larger than $110 \mu\text{m}^2$. However, the impact of the size of the effective area on the SSE-distance product was not very significant. The results also showed that the largest SSE-distance product could be achieved by using the QPSK format than the 16QAM or 64QAM format in the MCF link consisted of trench-assisted MCFs.

Acknowledgment

This work was supported by the IT R&D program of MKE/KEIT (10043383, Research of mode-division-multiplexing optical transmission technology over 10 km multi-mode fiber).